LBNL-2001009

ERNEST ORLANDO LAWRENCE
BERKELEY NATIONAL LABORATORY

Development of a Standard Test Method for Reducing the Uncertainties in Measuring the Capture Efficiency of Range Hoods

Yang-Seon Kim, Iain Walker, and Woody Delp

Energy Technology Area
March, 2017

Disclaimer

This document was prepared as an account of work sponsored by the United States Government. While this document is believed to contain correct information, neither the United States Government nor any agency thereof, nor The Regents of the University of California, nor any of their employees, makes any warranty, express or implied, or assumes any legal responsibility for the accuracy, completeness, or usefulness of any information, apparatus, product, or process disclosed, or represents that its use would not infringe privately owned rights. Reference herein to any specific commercial product, process, or service by its trade name, trademark, manufacturer, or otherwise, does not necessarily constitute or imply its endorsement, recommendation, or favoring by the United States Government or any agency thereof, or The Regents of the University of California. The views and opinions of authors expressed herein do not necessarily state or reflect those of the United States Government or any agency thereof or The Regents of the University of California.

Acknowledgements

This work was supported by the Assistant Secretary for Energy Efficiency and Renewable Energy, Building Technologies Program, of the U.S. Department of Energy under Contract No. DE-AC02-05CH11231.

1. Introduction

Cooking activities and residential cooking burners are a major source of pollutants of concern for health, such as PM2.5, nitrogen oxides (NOx), carbon monoxide (CO), formaldehyde (CH_2O), and ultrafine particles. Also, a high quantity of water vapor can be produced that is not a direct health concern but can contribute to high indoor humidity and related mold and pest issues. Combustion products from the natural gas used for cooking can cause a variety of respiratory health problems, such as asthma and allergies (Zhang et al. 2010; Long et al. 2000; He et al. 2004; Buonanno et al. 2009).

To protect the public health from risks of indoor pollutants, the World Health Organization (WHO) (WHO 2010), the California Ambient Air Quality Standards (CAAQS) (CalEPA 2013), the National Ambient Air Quality Standard (NAAQS) (U.S. EPA No date), and the California Office of Environmental Health Hazard Assessment (OEHHA)Monserrat 2016), have guidelines for upper limits of pollutant concentrations. Table 1 summarizes the standard guidelines for NO_2, CO, CH_2O and PM_{10} for one-hour exposure level.

Table 1. Summary of standards for indoor air pollutant level

Standard	NO_2 ($\mu g/m^3$)	CO ($\mu g/m^3$)	CH_2O ($\mu g/m^3$)	PM_{10} ($\mu g/m^3$)
WHO	200	35	100	NA
CAAQS	339	23	NA	20
NAAQS	188	40	NA	12
OEHHA	470	23	55	NA

Note: $\mu g/m^3$ stands for micrograms per cubic meter.

A range hood mounted over the cooktop is commonly used in residential buildings to reduce odors, moisture, and pollutants resulting from cooking activities. Several studies (Logue et al. 2013; Rim et al. 2012; Singer et al. 2012) have shown reductions in cooking-related indoor air pollutants due to range hood use. In simulation studies, range hoods have been shown to significantly reduce the frequencies of pollutant concentrations that exceed the health-based pollutant standards in homes (Logue et al. 2013), with NO_2 reductions of 51 to 15 percent, CO reductions of 6 to 2 percent, and CH_2O reductions of 24 to 11 percent. Particle concentration reductions of 31 to 94 percent for front burners and 54 to 98 percent for back burners have been demonstrated in laboratory studies (Rim et al. 2012).

A range hood is a requirement in several building codes for new homes, and the required airflow rates for range hoods are specified by indoor air quality standards. For example, ASHRAE Standard 62.2-2016 requires a minimum airflow rate of 100 cubic feet per minute (CFM) (50 liters per second, L/s) together with a sound rating of 3 sone or less (ASHRAE 2013) for range hoods. Existing standards use air flow as a metric of

interest when considering kitchen ventilation because air flow measurements are readily available and have been used as metric of performance for many years. Manufacturers quote air flow rates in product literature, and the Home Ventilating Institute maintains a directory of certified air flow rates for range hoods (HVI 2015). However, air flow alone does not tell us how much of the cooking pollutants are exhausted by the range hood. A much better performance metric is the capture efficiency (CE), defined as the fraction of pollutants emitted during cooking that are exhausted directly to outside. A CE of 100 percent means all of the cooking pollutants exhaust directly to the outside, and a CE of zero would have no pollutants directly exhausted, allowing all of them to mix with indoor air.

Existing test methods for commercial kitchen hoods use flow visualization techniques to check that the whole plume of pollutants from the cooktop is captured by the hood (ASTM 2005), i.e., a CE of 100 percent. Commercial hoods are then rated by the quantity of air required for 100 percent capture. However, that methodology is difficult to adapt to the estimation of residential range hood capture characteristics. For residential range hoods, it is highly impractical to require 100 percent capture—mostly due to the physical size of the hoods and the high flow rates (and associated mechanical make-up air and tempering systems) required to attain this level of performance. In addition, in homes it is less important to have 100 percent capture since there is much less cooking than in commercial kitchens. Therefore, when rating residential hood performance, the focus is on quantitatively determining the partial capture efficiency for the air flows and hood geometries that are appropriate for residential kitchen applications. This requires a different experimental approach than that used to rate commercial hoods. The fundamental concept for the new residential CE test method is that the plume of pollutants from a cooking event is seeded with a tracer gas. Measurements of tracer gas concentrations can then be used to determine CE.

Lawrence Berkeley National Laboratory (LBNL) developed an initial tracer gas technique for determining CE (Walker et al. 2016) and used it in previous laboratory and field studies (Singer et al. 2012; Walker et al. 2016). It showed that CE varied from 15 to 98 percent. This variation indicates that a test method is required to distinguish among the performance of different devices. Additional laboratory evaluations have shown that there can be issues regarding testing repeatability that require refinement of the test method if it is to be useful as a rating tool. For example, in one case, capture efficiency changed from 85 to 94 percent in the same test condition. The present study focused on making the test method more consistent and repeatable by examining parameters such as stability of tracer gas emitters, fluctuation of the air movement in the testing room, and position of the tracer gas emitters.

Development so far has been restricted to wall-mount range hoods, but future developments will include island and downdraft applications.

This test method is intended to be used as an ASTM test method to evaluate range hoods in a standardized way. Its development has included input from the ASTM working group responsible for writing the ASTM test method. This group includes range hood manufacturers, researchers, and potential users of the test method.

2. Test Method Outline

The test method uses a tracer gas to seed the hot plume above the heating elements on a cooktop placed in a test chamber. Measurements of tracer gas concentrations are used to calculate CE.

The range hood to be tested is mounted on a wall above a combined heat source and a tracer gas emitter. The plume size and spread depend on the initial source size and temperature and the power put into the plume, therefore, it is important to have the plume from the cooktop be similar in its geometry and air velocities to those during a cooking event. The heat source and emitter have been developed to have a specific size, power output, and surface temperature based on analyses of typical cooking events. Data on typical events was provided by members of the ASTM working group, primarily from market studies by manufacturers. More details of the selection of heat source and emitter characteristics are given in an earlier LBNL report on the development of a tracer gas capture efficiency test method (Walker et al. 2016).

Carbon dioxide was chosen as a tracer gas for safety and cost reasons. A flow meter, iris damper, and auxiliary fan were used to measure and control the air flow through the range hood. Although the air flow measurement is not needed for CE calculations, it is important that air flows be known, controlled, and recorded during the testing for consistency.

The tracer gas concentration is measured in three locations: inside the test chamber (C_c); at the test chamber inlet (C_i); and in the exhaust ducting (C_e). The concentrations are averaged for a period of 10 minutes after reaching steady state to minimize the effect of the temporal variability in the tracer gas concentration.

The CE is given by:

$$CE = \frac{C_e - C_c}{C_e - C_i} \qquad (1)$$

Equation 1 is based on an assumption of steady-state concentrations. Although it is possible to reformulate this relationship to include time-varying concentrations, additional uncertainties are introduced. For a standardized test method, the additional testing time required to wait for steady state is a reasonable trade-off to make in a laboratory test that is intended to produce reliable and consistent ratings with minimal uncertainties. The analysis represented by Equation 1 has distinct advantages. It is a ratio of two concentrations differences, where the numerator is the difference between the concentration in the test chamber and the exhaust, and the denominator is the difference between the air inlet to the testing chamber and the exhaust. Therefore, any measurement bias would effectively be canceled out, as it would be roughly equivalent above and below the divisor. When determining if the test has achieved steady state,

we use the metric of test chamber air changes. The number of air changes is the total volume of air moved through the test chamber by the range hood in a given time divided by the test chamber volume. The minimum time to reach steady-state conditions is calculated using Equation (2):

$$t = \frac{n * V_{Chamber}}{Q_{air}} \quad (2)$$

The previous work done by LBNL analyzed time series of measured tracer gas concentrations to create five-minute time averages (Walker et al. 2016). Steady state was assumed to be reached if the difference between consecutive time averages was less than 5 percent. In most cases four chamber-air changes were observed to be required. However, this was not always consistent, and sometimes up to eight chamber-air changes were required to reach to the steady-state condition. Detailed analysis of the time series concentration data indicated that these longer times were likely due to variations in tracer gas concentrations separate from the gradual approach to steady-state conditions. This study investigated this in more detail.

2.1. Test Chamber and Apparatus Development

This study uses the same test chamber that was used for the previous LBNL study (Walker et al. 2016). It was designed to be representative of a small residential kitchen. Figure 1 shows a schematic of the tracer gas and air flow control apparatus. Figures 2, 3, and 4 show the cabinetry used in the test chamber, together with tracer gas measurement locations. It is important to specify the location and geometry of the kitchen cabinetry because the cabinetry changes flow patterns in the room, and the cabinets to either side of the range hood directly influence flow patterns above the cooktop. The test chamber has an air inlet on the ceiling with a diffusing plate and an exhaust duct which is connected to the range hood. The floor of the test chamber is approximately 4.57 meters (m) (15 feet [ft]) x 2.29 m (7.5 ft), and the walls are 2.44 m (8 ft) high, so the chamber has a volume of 25.49 cubic meters (m^3) (900 cubic feet [ft^3]).

Since CO_2 is used as a tracer gas, the concentration of tracer gas in the air can enter the chamber. Therefore, it is necessary to seal the test chamber to ensure that most of the air comes to the chamber, to make up for the range hood exhaust, came through a known inlet where the concentration of tracer as is measured (C_i). The test chamber was thoroughly sealed to a tightness of 2.5 air changes at 50 pascals (Pa). Given a 25.4 centimeter (cm) (10 inch [in.]) diameter air inlet, approximately 94 percent of air entering the test chamber comes through the air inlet.

The CO_2 concentrations are measured using PP Systems SBA-5 analyzers that have an accuracy of ± 1 percent (±25 parts per million [ppm]) of the calibrated range. Daily calibration checks were made with pre-mixed bags of air and tracer with known concentrations of 2,466 ppm, 1,726 ppm, and 986 ppm. These concentrations cover the

range of tracer gas concentrations measured during the experiments. The tracer gas injection rate was adjusted depending on the air flow through the range hood such that the steady-state concentration in the exhaust duct was about 2,000 ppm (about 1,500 ppm above ambient). This was selected to be in the center of the range for the CO_2 monitoring equipment. The injected CO_2 flow rate is controlled by a mass flow controller with an accuracy of ± 1 percent. The required tracer gas flows were in the range of 0.15–0.3 L/s, or about 0.2 percent of the total system air flow through the range hood.

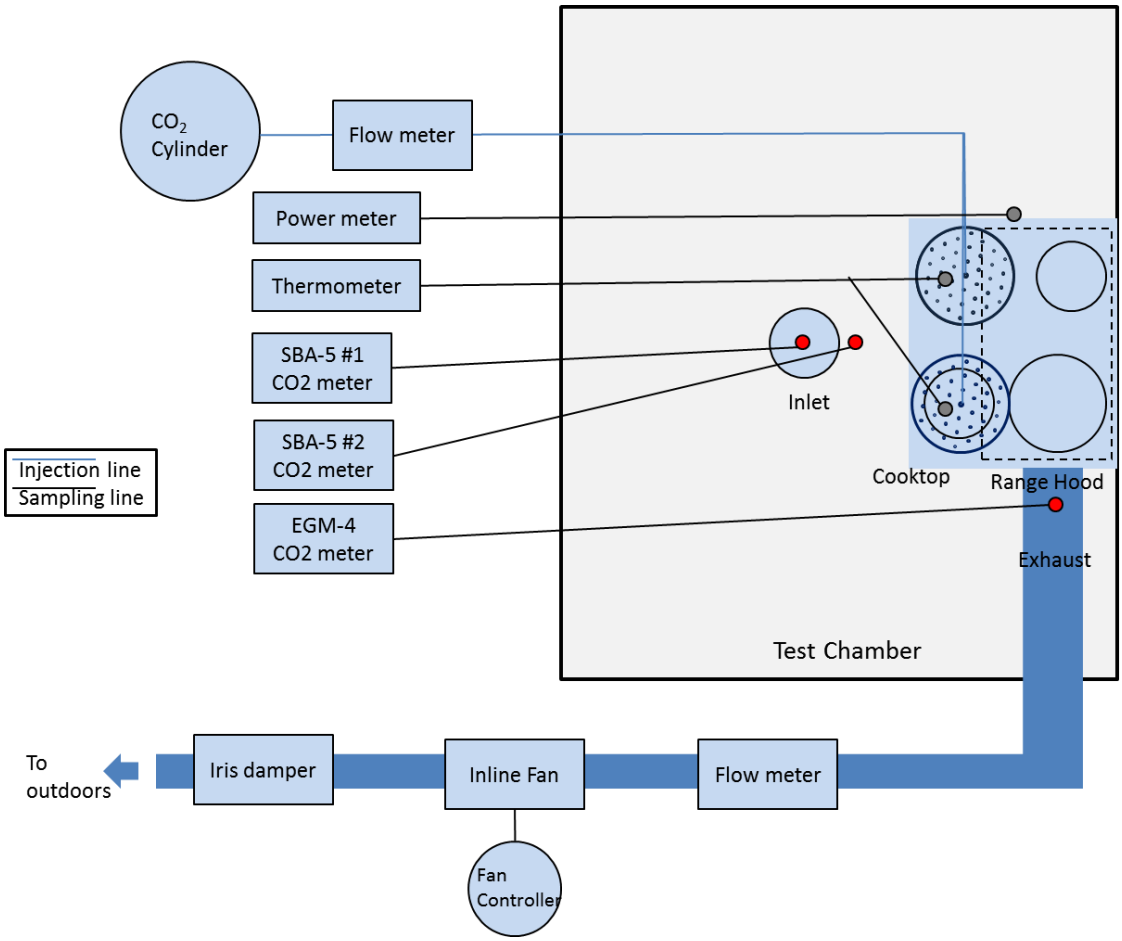

Figure 1. Schematic of the capture efficiency test chamber

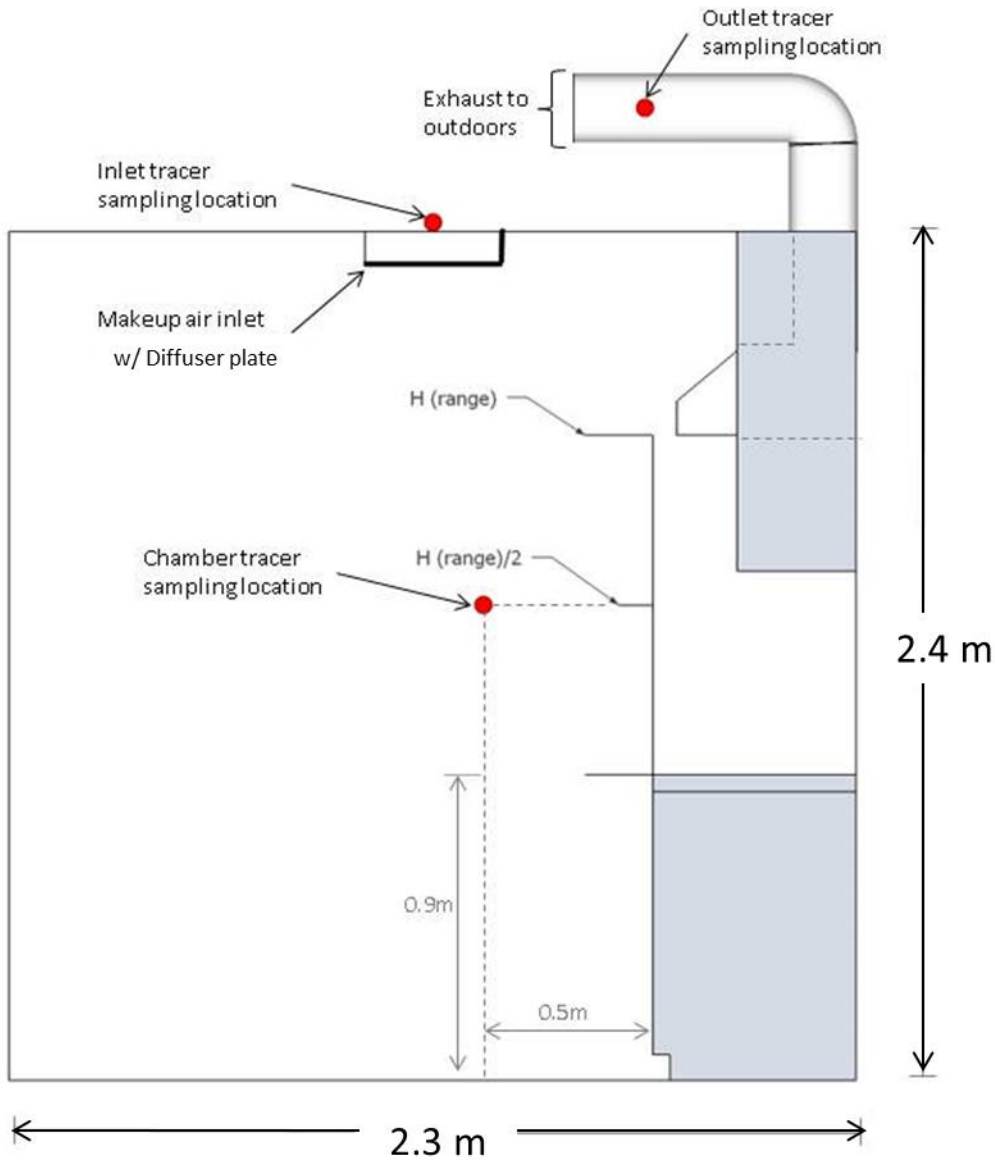

Figure 2. Sketch of an example test chamber (section), H: height

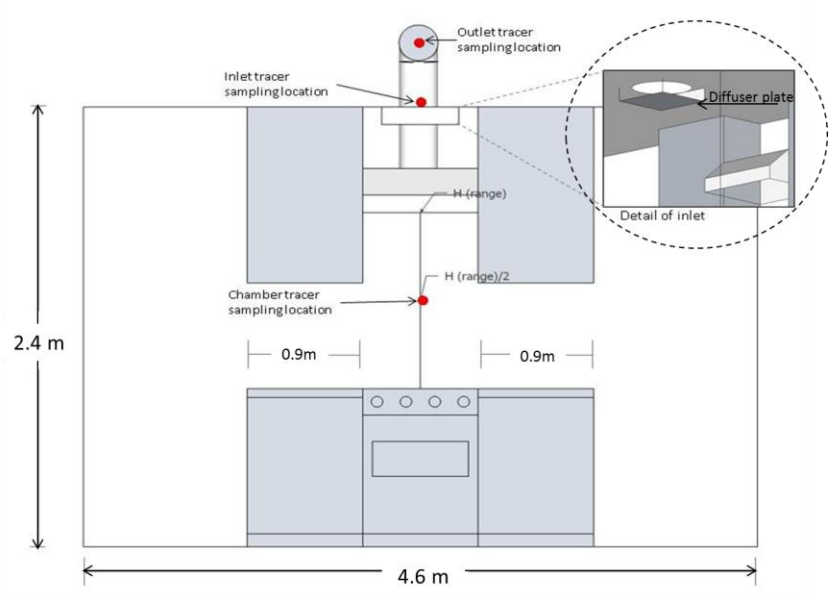

Figure 3. Sketch of example test chamber (elevation)

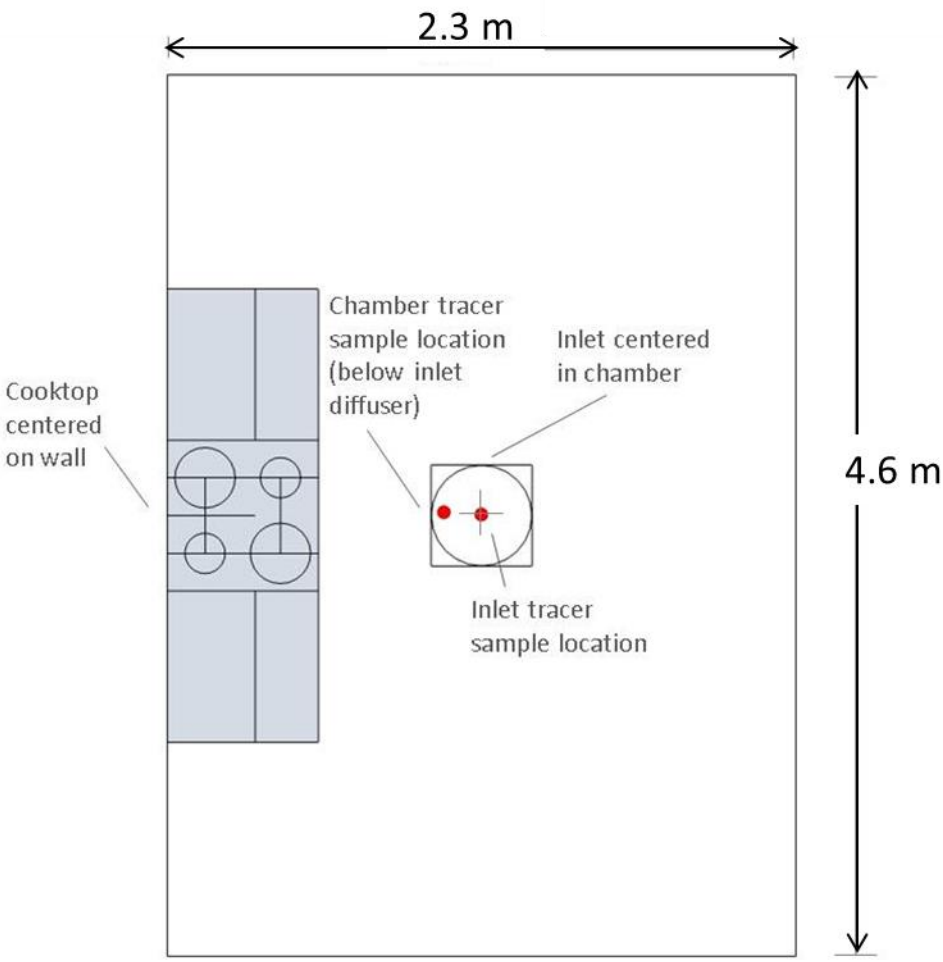

Figure 4. Sketch of example test chamber (plan)

The range hood outlet was connected to a 22 cm (8.7 in.) diameter duct that exited the chamber through the ceiling. A variable-speed inline fan and an iris damper were installed to control the air flow of the range hood with an accuracy of ± 2.5 L/s (5.3 CFM).

Previous LBNL testing measured the tracer gas concentration at multiple points in the test chamber to determine the representative location of the tracer gas concentration in the air entering the plume (Walker et al. 2016). The current study repeated these multi-point tracer gas concentration measurements to ensure that changes to the test procedure (e.g., emitter design and location) did not change this optimum location. The room tracer gas concentration (C_c) is measured on the cooktop centerline, 0.5 m (20 in.) into the room from the cooktop, and vertically halfway between the cooktop and the bottom of the range hood.

The cooktop was located in the center of the long walls of the chamber. A four-element electric range 76 cm (30 in.) wide, 65 cm (25.5 in.) deep, and 90 cm (35.4 in.) tall was

used instead of natural gas burners, for safety and ease of power measurement. Figure 5 shows the schematic of the heating elements on the cooktop, which has two 14 cm (5.5 in.) diameter heating elements with 1,250 watts (W) power capacity and two 17 cm (6.7 in.) diameter heating elements with 2,100 W power capacity. Based on input from the ASTM Working Group and equipment manufacturers, two burners were used—each operating at 1,000 W. The power was monitored using an ELITEpro XC™ Energy Logger with an accuracy of ± 0.2 percent. Some tests used one back and one front burner, and other tests used two front burners.

Figure 5. Schematic of the heating elements on the cooktop

Tracer gas emitters were specifically designed to maintain an upper surface temperature of 200°C ± 5°C (392°F ± 9°F). The surface temperature of the tracer gas emitters was measured using K type Watlow contact thermocouples with an accuracy of ± 2.2°C (4°F).

The tracer gas concentrations, heating element power consumption and surface temperatures, and range hood air flows were recorded every two seconds and averaged every minute to observe temporal fluctuations, to enable the research team to evaluate averaging times and determine steady state.

The current study addressed two issues that were found to cause test uncertainties: (1) fluctuations of the air movement in the chamber and (2) repeatability problems with previous versions of tracer gas emitters.

2.2. Changes in the New Test Method

2.2.1. Air Movement in the Test Chamber and Chamber Air Inlet Design

During development of the test method, we found that CE varied from 85 percent to 95 percent in the same test condition (129 L/s [273 CFM], a 61 cm [24 in.] range hood mounting height from the cook top). Therefore, we tried to identify the exact cause for these fluctuations. First, we assumed that the CE could be changing with the tracer gas injection rate. Ideally, the tracer gas injection rate represents the level of air pollutant generated from the cooking activities; therefore, it did not seem likely that it would be a problem that would change the CE of the testing range hood.

The second parameter we suspected of causing this fluctuation was the range hood air flow. When the range hood delivers high air flow from the room to outside, the air inlet delivers make-up air to the testing chamber, and we thought the high airflow rate may possibly cause an air flow pattern in the testing chamber that could affect capture efficiency. Therefore, we tested the CE in a different air inlet configuration to see if it would reduce the CE variance.

Figure 6 shows the detail of original air inlet, which was a 25.4 cm (10 in.) diameter opening located in the chamber ceiling. Located 4.5 cm (1.8 in.) below the ceiling, a 30.5 cm x 30.5 cm (12 in. x 12 in.) diffusion plate was used to prevent inlet air from blowing directly on the range hood and cooktop. The diffusion plate was blocked on the side that faced the cooktop/range hood but was open on the other three sides.

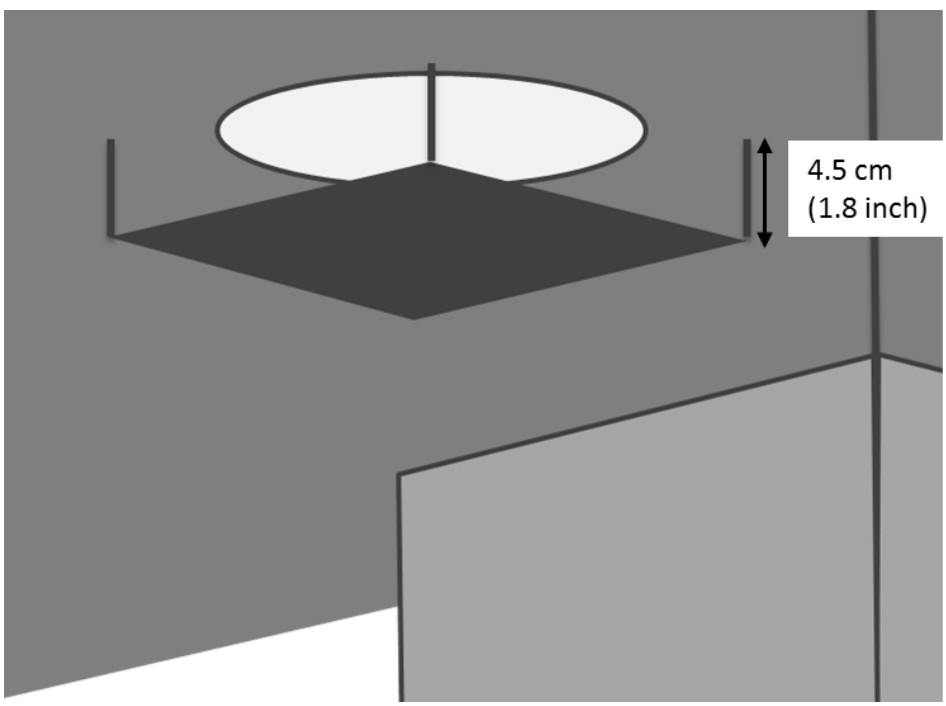

Figure 6. Detail of air inlet with diffuser plate (original version used for previous LBNL testing method)

With the old air inlet, we performed the CE test with different tracer gas flow rates. For each test, we injected tracer gas at a rate of 2,000 ppm, and we increased the rate to 3,000 ppm to check whether it would cause a difference in the CE results. These test conditions were the same as those in previous tests. We repeated the tests to see if the results were replicable; four times at 2,000 ppm and three times at 3,000 ppm. To check whether the tracer concentration changes over the chamber, multiple locations were used to collect the tracer concentrations.

Figure 7[1] shows the time-varying capture efficiency at a high flow rate with the original air inlet. An initial transient can be observed, but after four air changes there were still considerable fluctuations with periods of about 10 to 20 minutes. This is not simply noise in the concentration signal—it is a fundamental change in CE due to air flow patterns in the test chamber.

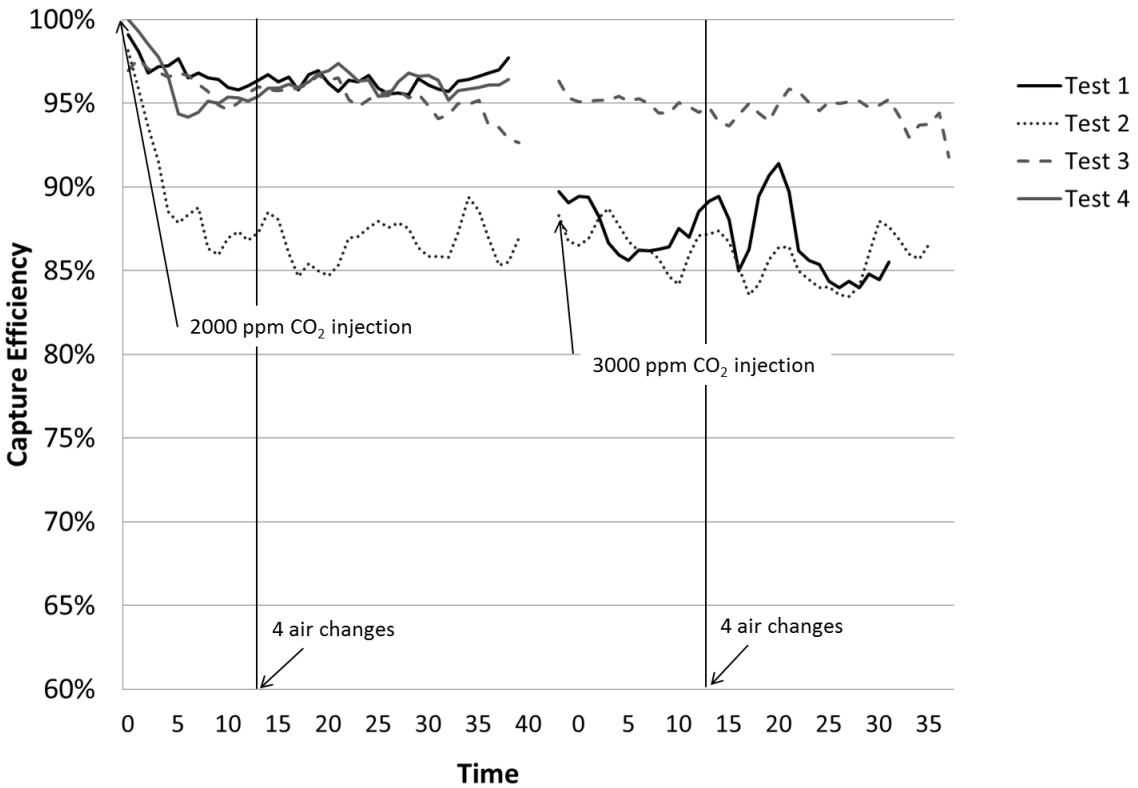

Figure 7. Capture efficiency results with the old inlet, at an air velocity of 129 L/s (273 CFM), a 61 cm (24 in.) range hood mounting height, a 4.5 cm (1.8 in.) distance of the diffuser plate from the ceiling, two new emitters, and two fronts.

The results illustrate that the repeatability due to these fluctuations was unacceptably large, with CE varying from 85 percent to 95 percent. To check whether the tracer

[1] The tests were performed with new emitters on two front burners, 24 in. range hood mounting height with a 129 L/s (273 CFM) range hood airflow.

concentration changes over the chamber, multiple locations were used to collect the tracer concentrations. This fluctuation was found to be present in all locations, and the concentrations rose and fell together at all locations in the test chamber.

These results imply that there are changes in air flow pattern in the room that change the capture efficiency. When the high flow of air hits the diffusion plate, an air jet is created. This periodic variability in test results was observed most strongly at higher air flow rates. This led us to believe that specific flow patterns that depended on air flow velocities in the test chamber were being set up in the test chamber.

The air jet discharging parallel to the ceiling could lead to a jet of air staying at the ceiling rather than entering the room due to the Coanda effect (a phenomena in which a jet flow attaches itself to a nearby surface and remains there)—particularly at higher air flows. In general, the Coanda effect could result in high-velocity jets circulating in the test chamber (HVI 2015; Zhang et al. 1990). This effect has a significant impact on the CE results (as demonstrated by fluctuating results, even under the same testing conditions). At lower velocities, the air momentum is insufficient to create the Coanda effect or for jets to persist in the room, and the inconsistent results are not observed.

To confirm that the jet air flow discharging from the ceiling causes the testing chamber airflow patterns, additional measurements were performed with velocity probes (TA-5 Thermal Anemometer and accuracy ± 2 percent of velocity ranges). Measurements with hand-held anemometers showed that the highest velocities are at the air inlet. We found air velocities of 3m/s (592 feet per minute [fpm]) at the diffuser plate and 1 m/s (197 fpm) at the ceiling at 80 L/s (161 CFM) exhaust flow (which was one of the higher velocities we have tested). With the original shallow air inlet (4.5 cm [1.8 in.]), air velocities were as high as 0.6 m/s (120 fpm) in the jet of air at the ceiling near the wall opposite the range hood (the jet of air traveled across the ceiling from the air inlet to the wall opposite the range hood). More details are given in Appendix A.

These velocities introduce strong air flow patterns relative to those in the vicinity of the cooktop and induced in the thermal plume, which are typically less than 0.5 m/s (98 fpm).

Based on those results, we decided to reduce the air velocities entering the chamber and make the air entry more uniform. An ideal solution might be to uniformly distribute small holes over a wall or ceiling, but the construction of the test chamber, and the need to use the test chamber for other experiments, precluded this approach (although we may use it in the future). Another challenge in using a diffuse wall or ceiling is in ensuring a good measurement of incoming air tracer concentration.

For this second test, we dropped the bottom diffuser plate from its original 4.5 cm (1.8 in.) from the ceiling to 25 cm (10 in.) from the ceiling. Figure 8 shows this second version of the air inlet.

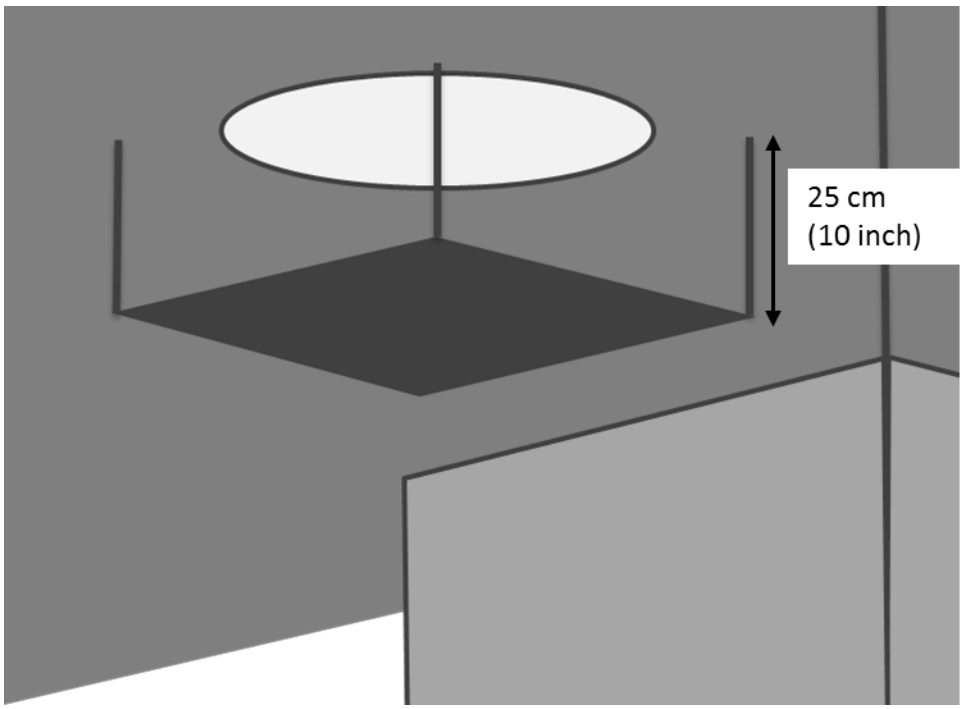

Figure 8. A detail of the second version of the air inlet, with the bottom diffuser plate placed 25 cm (10 in.) from the ceiling

Velocity measurements were taken again, with the new configuration. With the plate dropped to 25 cm (10 in.) from the ceiling, the jet of air entering the room was not uniform—it had higher velocities at the plate than at the ceiling. The resulting axial velocities were 1.5 m/s (295 fpm) (at 80 L/s [161 CFM] [80 L/s]) and 2.8 m/s (551 fpm) (at 129 L/s [273 CFM]) at the plate. Although the high velocity jet was moved away from the ceiling, the possibly of having jets within the room was still a concern.

Figure 9 shows the time-varying capture efficiency at the high flow rate with this second air inlet configuration. As with the first air inlet, tests were repeated several times and were performed at two tracer gas flow rates targeting tracer gas exhaust concentrations of 2,000 and 3,000 ppm. The CE varied from 96 percent to 99 percent, and the CE did not change due to tracer gas injection rate changes.

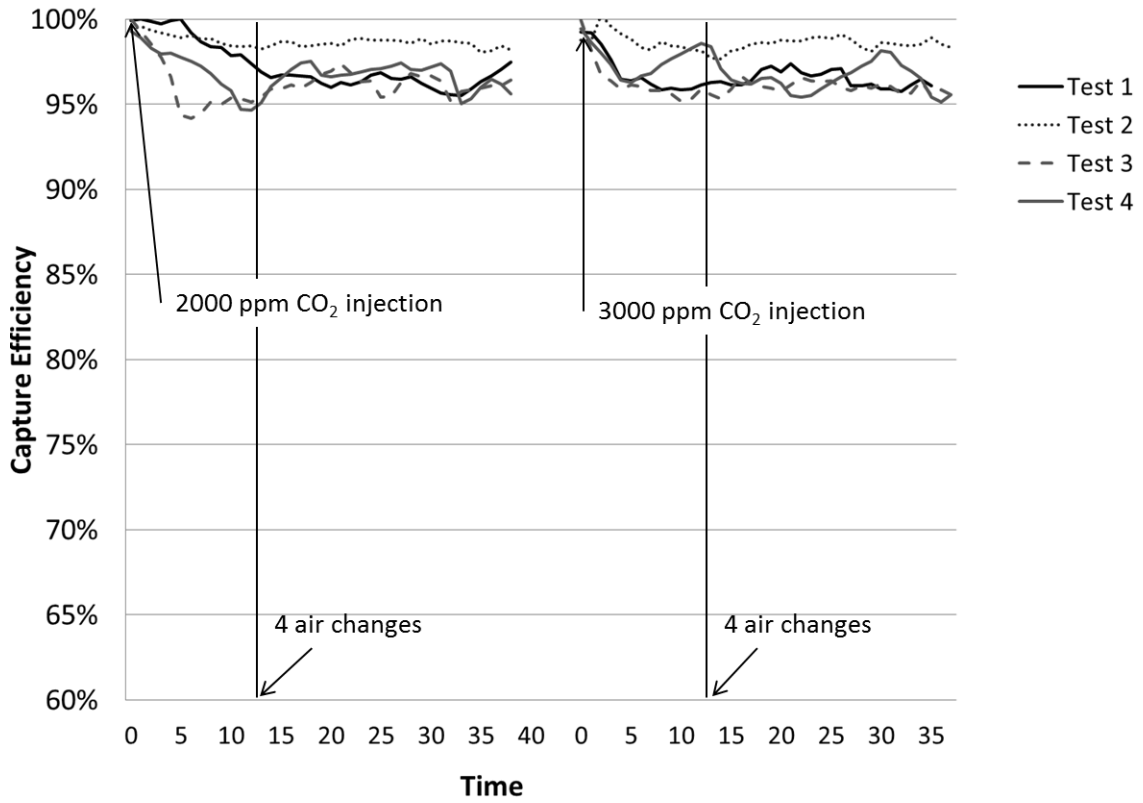

Figure 9. Capture efficiency results with the second version of the air inlet, at an air velocity of 129 L/s (273 CFM), a 61 cm (24 in.) range hood mounting height , a 25 cm (10 in.) distance of the diffuser plate from the ceiling, two new emitters, and two fronts

As had been done with the original air inlet, for the second inlet, the test chamber tracer gas concentrations were measured in several locations to attempt to observe any fixed flow pattern effects in the test chamber. Figure 10 shows the extra locations that were monitored using Vaisala CARBOCAP® Carbon Dioxide Transmitter GMW115 with an accuracy of ± 40 ppm. The red dot indicates the standard location specified in the draft test procedure, and the blue dots indicate additional locations.

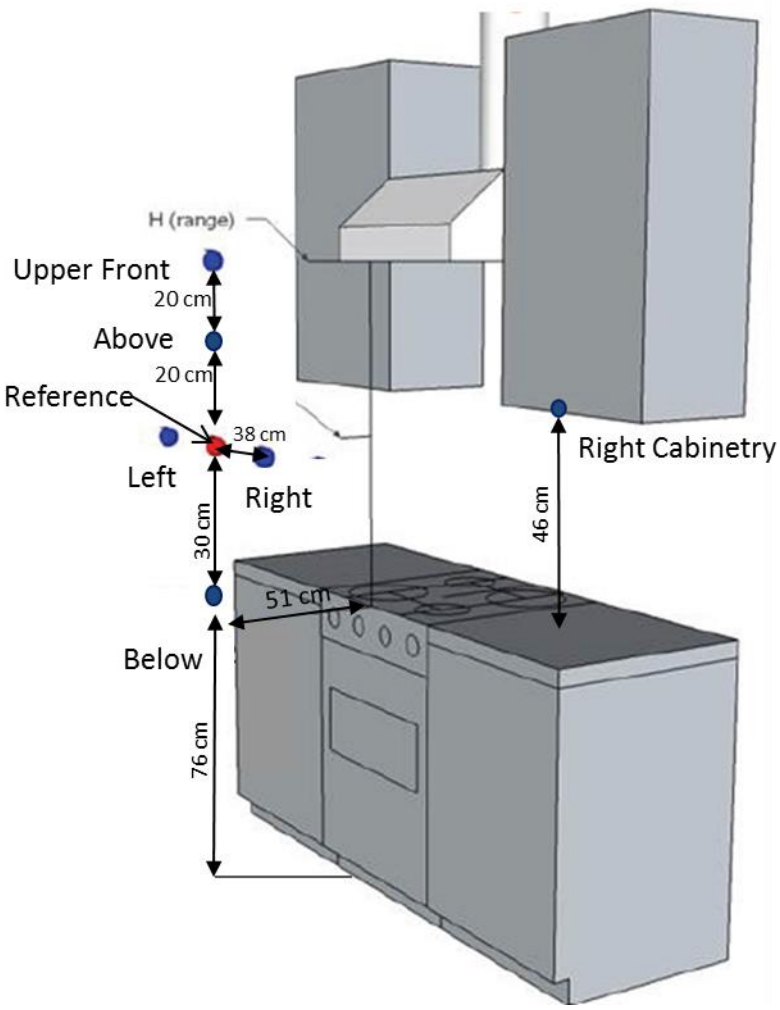

Figure 10. Multiple sampling locations in the chamber

Figure 11 shows the tracer gas concentrations from multiple sampling locations for the original and new air inlets. For the original air inlet most locations are similar, with the exception of the location measured on the far right of the cabinets. The new inlet does not show this discrepancy. However, these results for the new inlet still show some significant temporal variation, indicating that further improvement may be necessary.

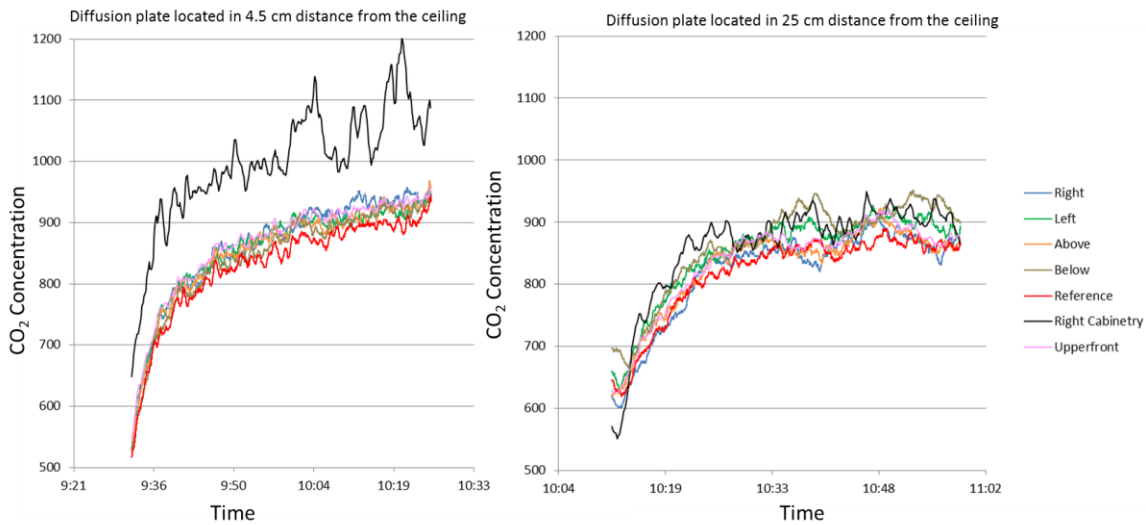

Figure 11. Tracer gas concentrations at multiple sampling locations, (left: 75 L/s (161 CFM), old air inlet, 61 cm (24 in.) mounting height, 2 fronts; right: 75 L/s (161 CFM), 25 cm diffusing plate, 61 cm (24 in.) mounting height, 2 fronts)

To make the air enter the room at a lower, more uniform velocity, a circular diffuser was installed in the inlet opening and a box was installed whose sides are made from MERV 11 filters below the inlet, as shown in Figure 12. The box has a closed bottom, and the side facing the cooktop/range hood is also closed, to prevent direct air flow in toward the range hood. This configuration has the double effect of lowering incoming velocities and introducing the air over a large area rather than in jets close to the ceiling. The diffuser box has sides 30 cm (12 in.) long. The measured air velocities were reduced to the 0.5 to 1.0 m/s (98 to 197 fpm) range, and the flow is no longer concentrated at the ceiling, thus avoiding the Coanda effect. The details of this result are shown in Appendix B.

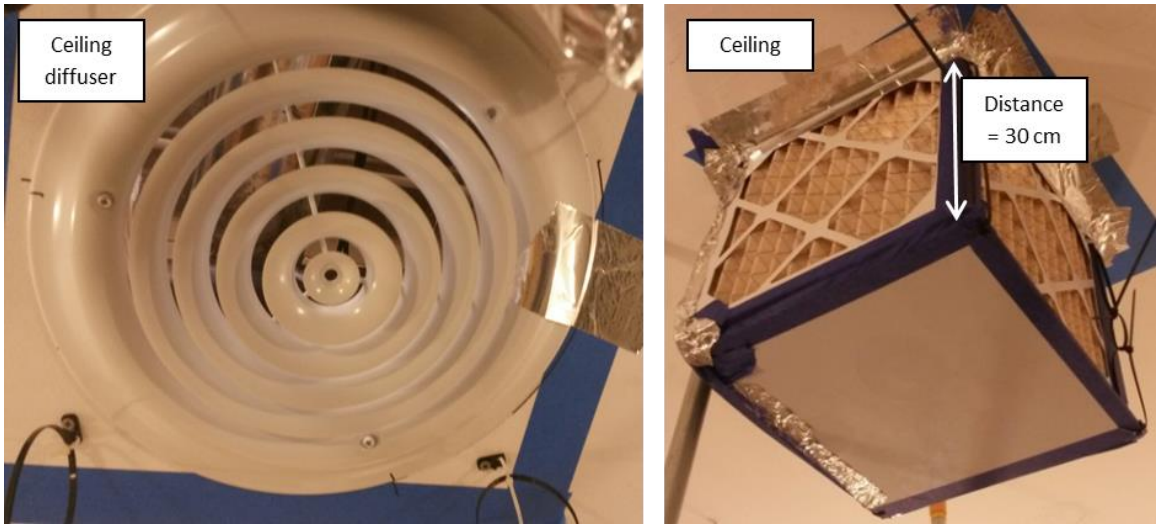

Figure 12. Detail of the new version of the air inlet (with a ceiling diffuser and MERV 11 air filters)

2.2.2. Tracer Gas Emitters

Figure 13 shows the set of tracer gas emitters which were developed from a previous LBNL study (Walker et al. 2012). The emitter assembly has four parts: a 28 cm (11 in.) diameter heat diffusion plate, a spacer to separate the heat diffusion plate from the 23 cm (9 in.) diameter pan, and perforated copper coils. The perforated copper coils were connected to the tracer gas controller to inject the tracer gas through small holes in the copper tubing. This approach effectively seeded the plume above the pans, but it might not effectively seed the entire plume. There is a contribution to the plume from the hot air that comes off the burner and travels around the edges of the pot or pan. In addition, these emitters may be difficult to replicate exactly in other environments or test conditions. Therefore, new tracer gas emitters were developed that use machined plates that can be accurately reproduced, and which can inject the tracer gas over the whole plume to include both the plume directly from the top of the pan and the plume coming from the burners around the sides of the pot or pan.

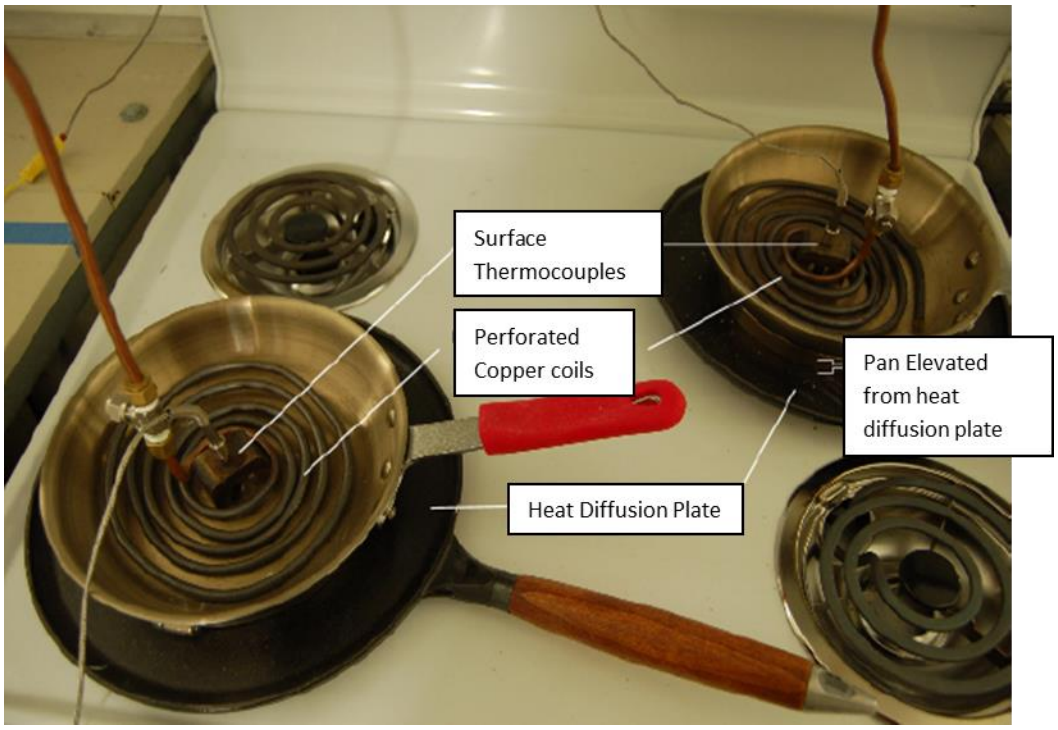

Figure 13. Tracer gas emitters (old version)

Figure 14 shows the new version of the tracer gas emitters. Figure 15 shows the parts that are required to assemble the tracer gas emitter: plate 1 is the upper tracer gas emission plate with 36 holes evenly distributed over the plate, plate 2 is a tracer gas reservoir with 18 holes on the bottom, plate 3 is a heat diffusion plate. All three plates are machined from aluminum. A set of 12.7 mm (0.5 in.) ceramic standoffs are used to separate the upper injector plate from the solid bottom plate. The new emitters are 25.4 cm (10 in.) in diameter. The holes on the bottom of plate 2 seed the air plume that flows around the upper plate, mimicking flow around a pot or pan above a burner. Ceramic standoffs between plate 2 and plate 3 work as barriers to reduce the direct heat conduction from the diffusion plate to the tracer gas emission part. This allows for the emitter plates to have the correct target power input (1,000 W/plate) while maintaining an upper surface temperature of 200°C (392°F). Without the standoffs the temperatures are much higher (290°C [554°F]) at 1,000 W input and are no longer realistic as a representative cooking temperature. The emitters were tested for leakage using a liquid leak detector solution that showed zero leakage at the tracer gas pressures used in the testing (just a few pascals).

Because the surface temperature is only monitored in one location it is important to know if this is representative of the whole plate. Figure 16 shows an infrared camera picture illustrating the uniformity of the surface temperature. Because of the temperature limits of the IR camera, this test was done at a surface temperature lower than that used during capture efficiency testing.

Figure 14. Tracer gas emitters (new version)

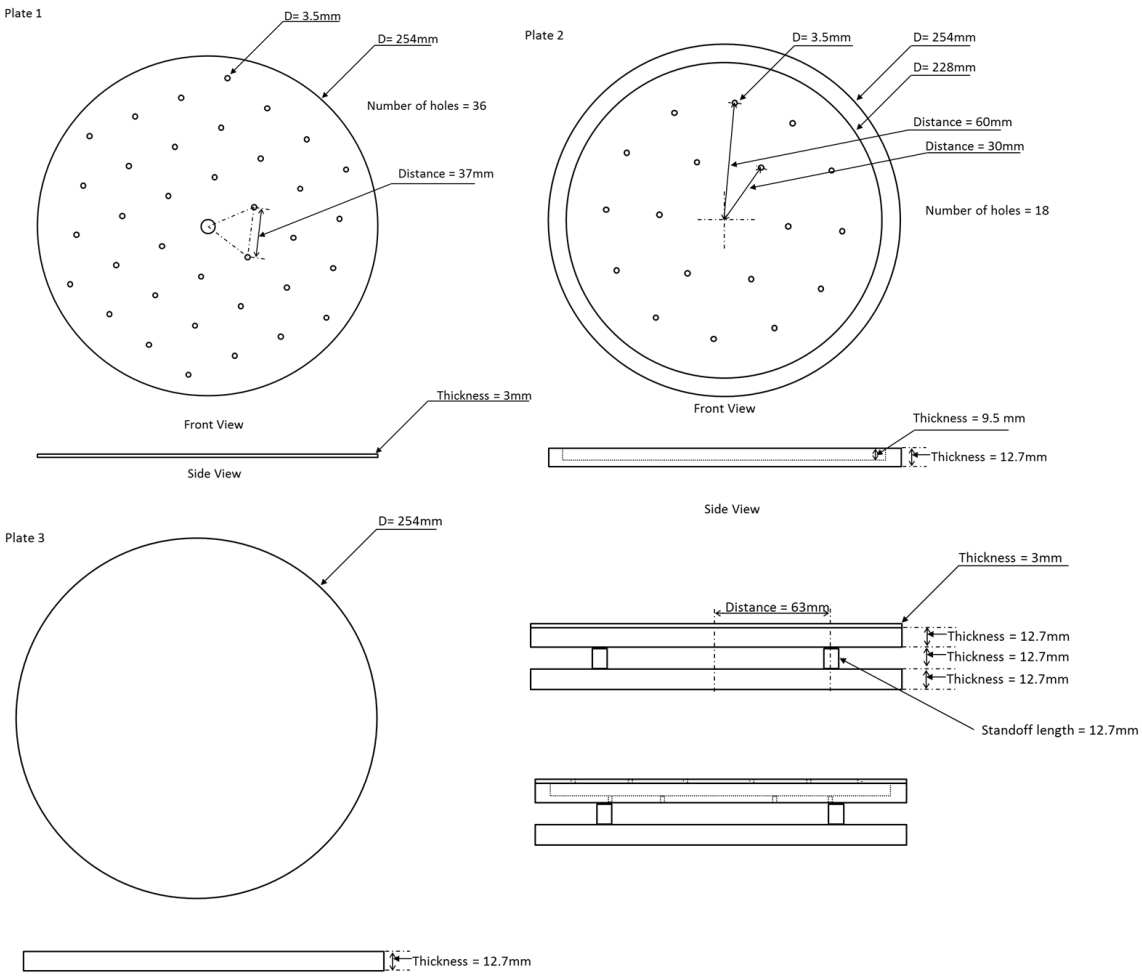

Figure 15. Schematic of new tracer gas emitters

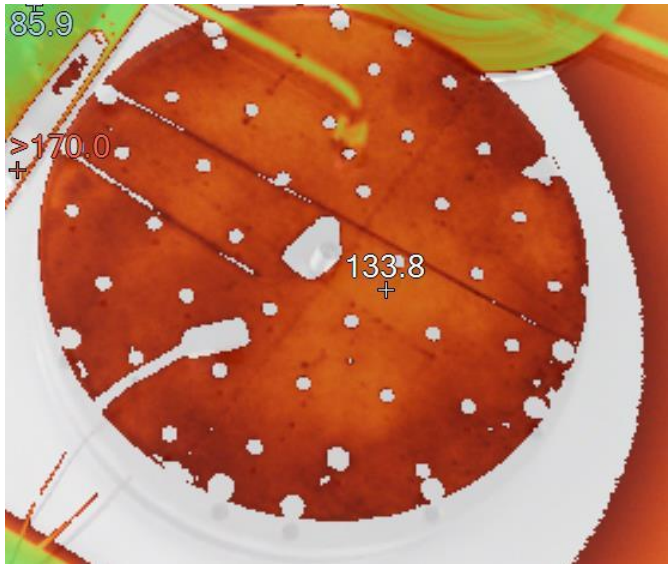

Figure 16. Surface temperature of a new tracer gas emitter

3. Results

Two range hoods were used for this test: a low flow/capture range hood (Broan 403001) and a high flow/capture range hood (Vent-a-hood B100). These extremes of high and low capture were used to ensure that the test method works equally well at these extremes. The following parameters were varied during these tests:

- New diffuse air inlet and old air inlet, to determine any biases between the two and establish repeatability of results using the new inlet.
- New emitters and old emitters, to determine any biases between the two and establish repeatability of results using the new emitters.
- Position of tracer gas emitters/hot burners (two fronts vs. one front and one back). The change from front and back to two fronts was requested by the ASTM task group. These tests will determine the magnitude of CE change resulting from this change.
- Different range hood mounting heights based on the manufacturer's recommendations
- Different air flow rate for the low flow/capture range hood (Broan).

Table 2 shows the test matrix with combinations of different conditions. In total, more than seventy unique test combinations were tested. Note that the test results shown in this section are our target test airflow (50 L/s [105 CFM], 76 L/s [161 CFM], and 129 L/s [273 CFM]). In the actual test condition, the measured airflow varied within 5 percent of our target test airflow. Summary characteristics of range hoods are given in Appendix C. Test results and details are given in Appendix D. The detailed step-by-step test procedures are given in Appendix E.

Table 2. Test Matrix

	Broan 403001 (Low Capture)				Vent-a-hood B100 (High Capture)	
Mounting Height	46 cm (18 in.)		61 cm (24 in.)		61 cm (24 in.)	69 cm (27 in.)
Old Emitters (Front and Back)	50 L/s (105 CFM)	76 L/s (161 CFM)	50 L/s (105 CFM)	76 L/s (161 CFM)	129 L/s (273 CFM)	129 L/s (273 CFM)
New Emitters (Front and Back)	50 L/s (105 CFM)	76 L/s (161 CFM)	50 L/s (105 CFM)	76 L/s (161 CFM)	129 L/s (273 CFM)	129 L/s (273 CFM)
New Emitters (Two Fronts)	50 L/s (105 CFM)	76 L/s (161 CFM)	50 L/s (105 CFM)	76 L/s (161 CFM)	129 L/s (273 CFM)	129 L/s (273 CFM)

3.1. Air Inlet

3.1.1. New Air Inlet

To examine the efficacy of the new diffuse inlet, Figures 17 a, b, and c show time series measurements of CO_2 and calculated CE for two front burners. These results show that four air changes is a reasonable time to wait for steady state for both the low and high capture scenarios.

To further check on reaching steady-state conditions, the standard deviation of the tracer concentrations and CE in the 10 minutes after four air changes was calculated. Table 3 summarizes the results. In all cases the standard deviation was less than 1 percent of CE and 0.5 percent was typical. Waiting longer before taking the ten-minute average did not reduce this standard deviation. As shown in Figure 17 c, the standard deviation of CE 20 minutes after four air changes was 0.9 percent. This is the same as the 10-minute results, indicating that four chamber air changes is adequate.

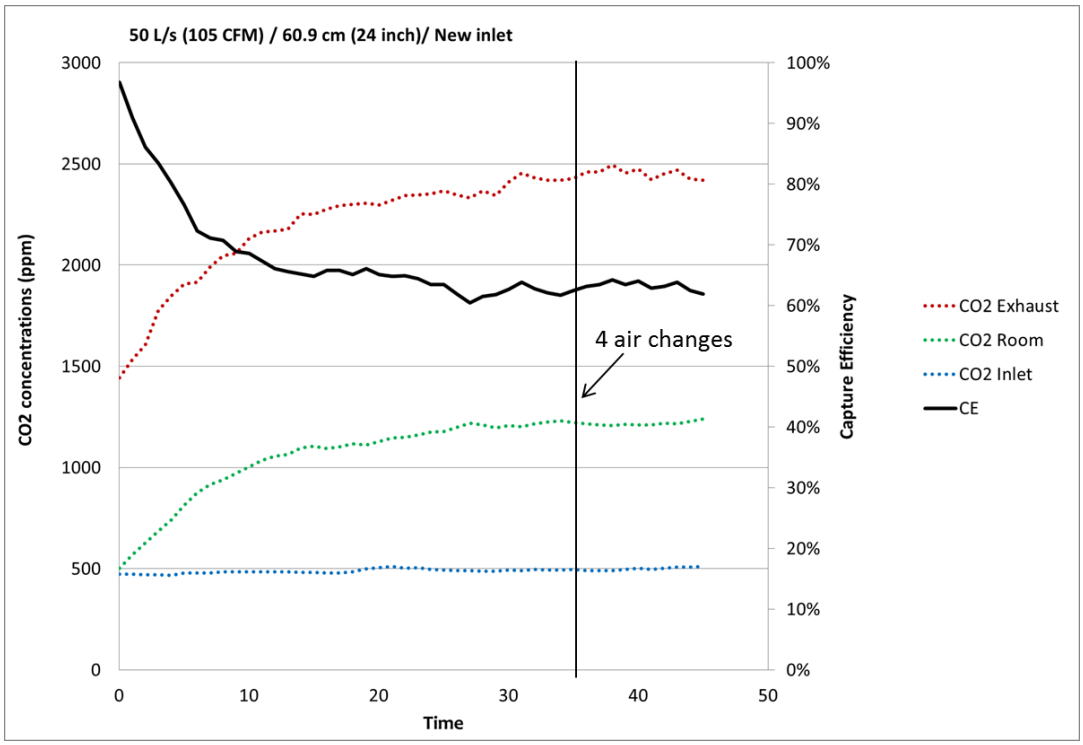

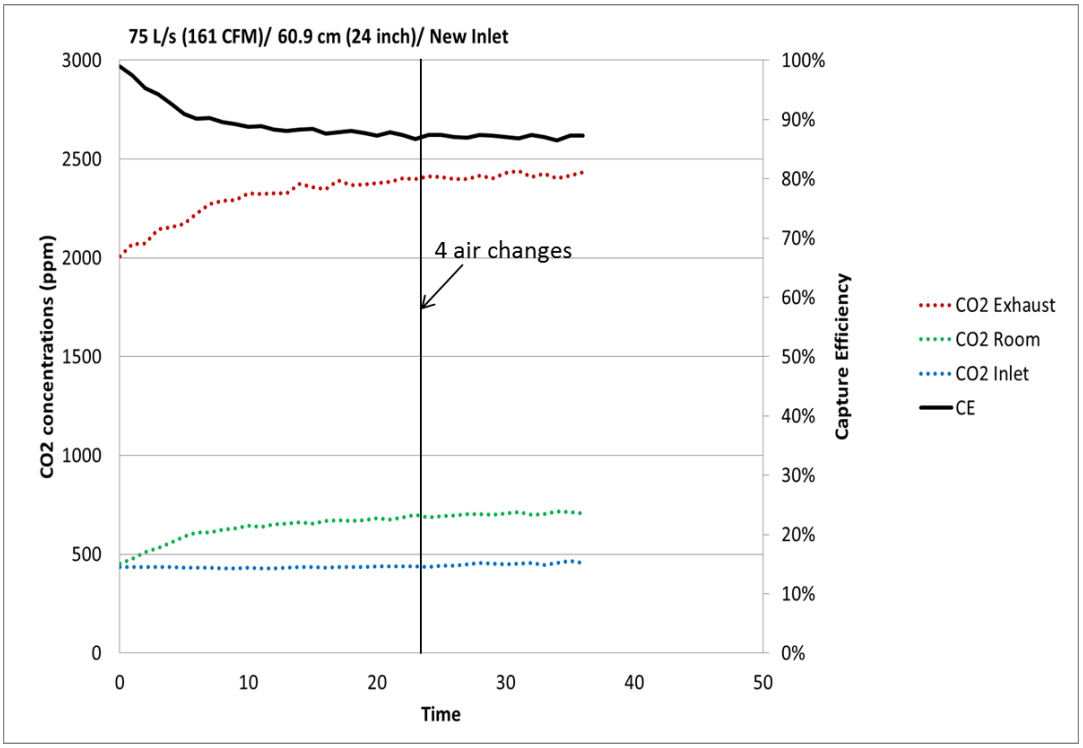

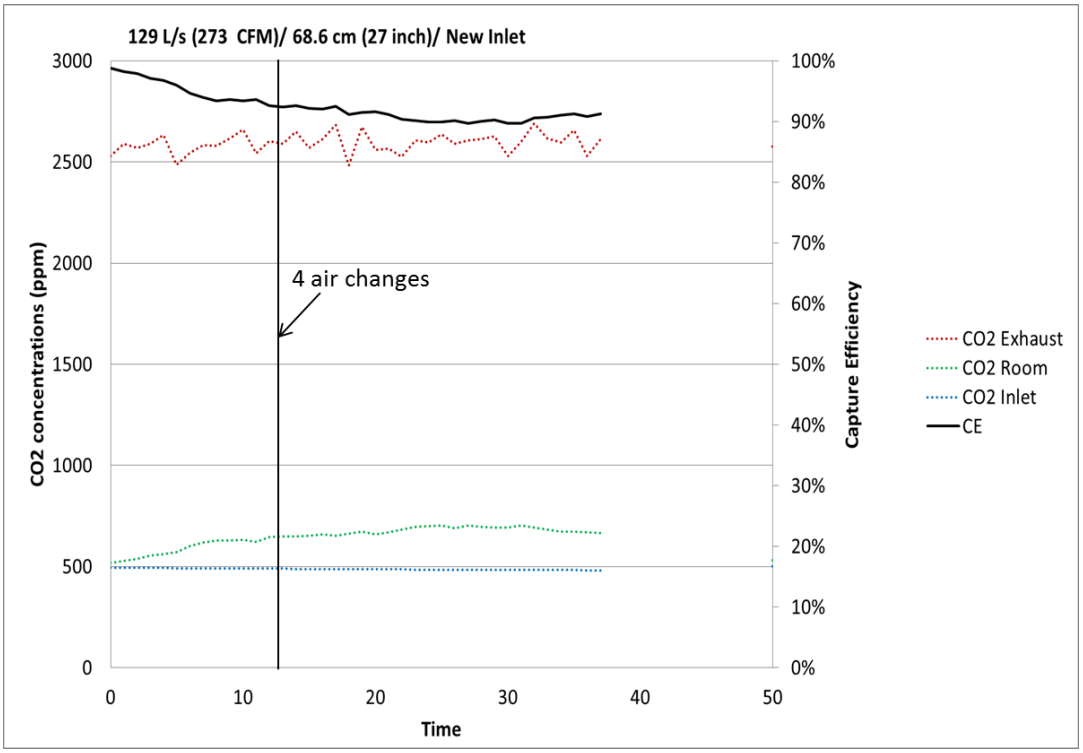

Figure 17. Capture efficiency with a new air inlet and tracer gas concentrations; (a) Broan range hood, 50 L/s (105 CFM), 61 cm (24 in.) mounting height, two fronts new tracer gas emitters; (b) Broan range hood, 75 L/s (161 CFM), 61 cm (24 in.) mounting height, two fronts new tracer gas emitters; and (c) Vent-a-hood, 129 L/s (273 CFM), 69 cm (27 in.) mounting height, two fronts new tracer gas emitters

Table 3 shows that the CE sometimes increases and sometimes decreases when comparing the old inlet results to the new ones.

In the cases of a high standard deviation of CE for the old inlet (that was indicative of jets formed by the air inlet) the new inlet always reduced the standard deviation. This, together with observations of the time series data above indicate that the new inlet gives more consistent results than the old inlet.

Table 3. Result summary comparing different air inlet conditions

Make	Model	Mounting Height (cm/in.)	Airflow (CFM)	Airflow (L/s)	Old inlet CE, mean and standard deviation	New inlet CE, mean and standard deviation
Broan	403001	46/18	161	75	89% (±0.3%)	89% (±0.5%)
Broan	403001	61/24	161	75	79% (±0.6%)	87% (±0.3%)
Broan	403001	46/18	105	50	70% (±0.6%)	65% (±0.9%)
Broan	403001	61/24	105	50	64% (±1.7%)	63% (±0.7%)
Vent-a-hood	B100	61/24	273	129	85%–96% (±2.5%)	95% (±1.4%)
Vent-a-hood	B100	69/27	273	129	83% (±1.6%)	91% (±0.9%)

3.2. Changing Emitter Location

Table 4 shows the results comparing a one front and one back emitter configuration to a two front emitter configuration. As expected, the CE is less for the two front emitter configuration. In addition, the range of results is greater for the two front emitter configuration (30 percent CE vs. 25 percent CE), with most of the changes at a lower CE.

Table 4. Result summary of changes of the tracer gas emitters' position

Make	Model	Mounting Height (cm/in.)	Airflow (CFM)	Airflow (L/s)	Two Fronts	Front and Back
Broan	403001	46/18	161	75	89% (±0.5%)	95% (±0.4%)
Broan	403001	61/24	161	75	87% (±0.3%)	92% (±0.4%)
Broan	403001	46/18	105	50	65% (±0.9%)	78% (±0.8%)
Broan	403001	61/24	105	50	63% (±0.7%)	74% (±0.7%)
Vent-a-hood	B100	61/24	273	129	95% (±1.4%)	99% (±0.3%)
Vent-a-hood	B100	69/27	273	129	91% (±0.9%)	99% (±0.5%)

3.3. Old emitters and new emitters

Table 5 compares the two emitter types tested, using one front and one back burner. For all configurations the new emitters have a higher CE. The changes are greater for the low CE cases, with more than a 10 percent increase in CE.

Table 5. Result summary comparing old emitters to new emitters

Make	Model	Mounting Height (cm/in.)	Airflow (CFM)	Airflow (L/s)	Front and Back (new emitters)	Front and Back (old emitters)
Broan	403001	46/18	161	75	95% (±0.4%)	88% (±0.6%)
Broan	403001	61/24	161	75	92% (±0.4%)	80% (±0.5%)
Broan	403001	46/18	105	50	78% (±0.8%)	65% (±0.7%)
Broan	403001	61/24	105	50	74% (±0.7%)	59% (±1.0%)
Vent-a-hood	B100	61/24	273	129	99% (±0.3%)	98% (±0.1%)
Vent-a-hood	B100	69/27	273	129	99% (±0.5%)	97% (±0.2%)

4. Summary

The combination of new emitter design and the use of a more diffuse air inlet improved the consistency of the test results. Using two front burners, the new diffuse air inlet, and 10-minute averaging, and waiting four chamber air changes for it to achieve steady state, gave repeatability uncertainties typically ± 0.5 percent CE, with ± 1.5 percent CE at worst.

The range of measured CE for the new emitter design and more diffuse air inlet on two front burners is from 65 to 95 percent for the two range hoods tested here.

Changing the tracer gas injection flow rate had an insignificant effect (less than 0.5 percent CE, which was below the experimental uncertainty).

Testing on two front burners rather than one front and one back lowered the CE by about 10 percent CE for lower CE and less at higher CE.

5. References

ASHRAE Standard 62.2 Ventilation and Acceptable Indoor Air Quality in Residential Buildings, ASHRAE, Atlanta, GA. 2013.

ASTM, "Standard Test Method for Capture and Contaminant Performance of Commercial Kitchen Exhaust Ventilation Systems. ASTM," 2005. [Online].

Buonanno, G., L. Morawska, and L. Stabile, "Particle Emission Factors During Cooking Activities," *Atmos. Environ.*, vol. 43, no. 20, pp. 3235–3242, Jun. 2009.

California Environmental Protection Agency, "Ambient Air Quality Standards (AAQS)." Jul. 2013.

He, C., L. Morawska, J. Hitchins, and D. Gilbert, "Contribution from Indoor Sources to Particle Number and Mass Concentrations in Residential Houses," *Atmos. Environ.*, vol. 38, no. 21, pp. 3405–3415, Jul. 2004.

HVI, Certified Home Ventilating Products Directory. Home Ventilating Institute publication 911. HVI, Morehead City, NC. 2015.

Logue, J. M., N. E. Klepeis, A. B. Lobscheid, and B. C. Singer, "Pollutant Exposures from Natural Gas Cooking Burners: A Simulation-Based Assessment for Southern California," *Environ. Health Perspect.*, Nov. 2013.

Long, C. M., H. H. Suh, and P. Koutrakis, "Characterization of Indoor Particle Sources Using Continuous Mass and Size Monitors," *J. Air Waste Manag. Assoc.*, vol. 50, no. 7, pp. 1236–1250, Jul. 2000.

Monserrat, L. "OEHHA Acute, 8-hour and Chronic Reference Exposure Level (REL) Summary," *OEHHA*, Jan. 2016.

Rim, D., L. Wallace, S. Nabinger, and A. Persily, "Reduction of Exposure to Ultrafine Particles by Kitchen Exhaust Hoods: The Effects of Exhaust Flow Rates, Particle Size, and Burner Position," *Sci. Total Environ.*, vol. 432, pp. 350–356, Aug. 2012.

Singer, B. C., W. W. Delp, P. N. Price , and M.G. Apte, "Performance of Installed Cooking Exhaust Devices," *Indoor Air*, vol. 22, issue 3, June 2012.

U.S. Environmental Protection Agency, "NAAQS Table." No date.

Walker, I. S., J. C. Stratton, W. W. Delp, and M. H. Sherman, "Development of a Tracer Gas Capture Efficiency Test Method for Residential Kitchen Ventilation," *LBNL-1004365*, Feb. 2016.

World Health Organization, "WHO Guidelines for Indoor Air Quality: Selected Air Pollutants," 2010.

Zhang, J. S., L. L. Christianson, and G. L. Riskowski, "Regional Airflow Characteristics in a Mechanically Ventilated Room Under Nonisothermal Conditions," ASHRAE Transactions, vol. 96, no.1, pp. 751-759, 1990.

Zhang, Q., R. H. Gangupomu, D. Ramirez, and Y. Zhu, "Measurement of Ultrafine Particles and Other Air Pollutants Emitted by Cooking Activities," *Int. J. Environ. Res. Public. Health*, vol. 7, no. 4, pp. 1744–1759, Apr. 2010.

Appendix A. Air velocity profile from the 25 cm (10 in.) gap inlet and 4.5 cm (1.8 in.) gap inlet

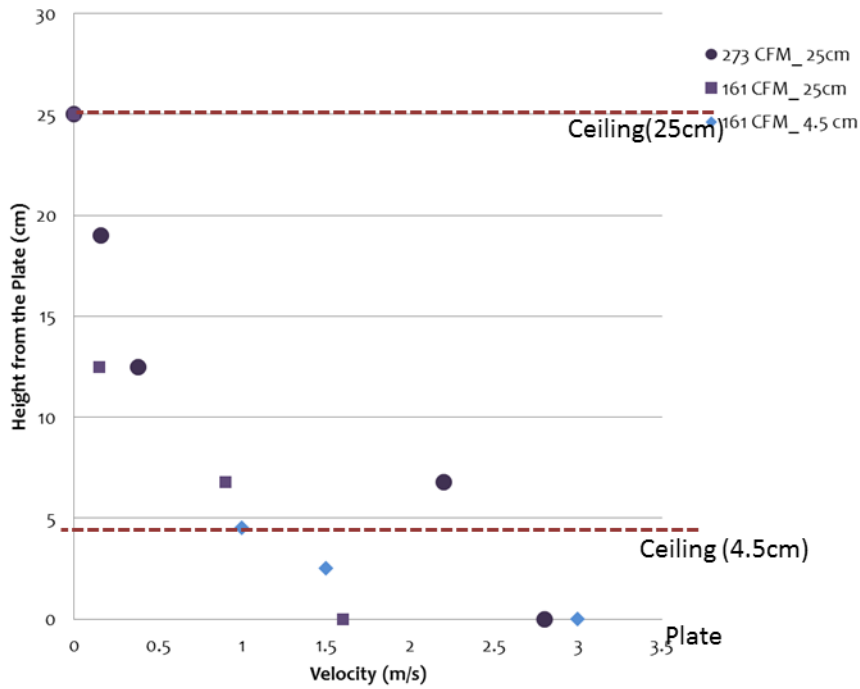

Figure A.1. Air velocity profile around the air diffusing plate with two different gap inlet

Air velocity profile from the ceiling depending on the distance (at a 25 cm [10 in.] gap inlet and 4.5 cm [1.8 in.] gap inlet) as below;

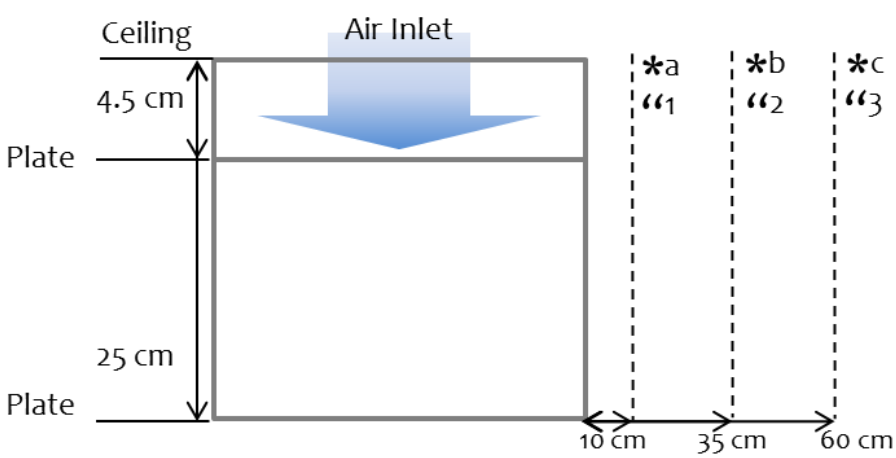

Figure A.2. A location of air velocity measurement

Table A.1 Air velocities at the location from Figure A.2.

Location	Velocity(m/s)
*a (4.5cm gap)	1.4
*b (4.5cm gap)	1.1
*c (4.5cm gap)	0.6
“1 (25cm gap)	0
“2 (25cm gap)	0
“3 (25cm gap)	0

Appendix B. Air Velocity Profile from the Inlet

Inlet air velocities were measured for the new diffuse inlet at the following locations:

a) *a, *b, *c, *d, *e: 10 cm (3.9 in.) away from the air filter surface. Measured locations were marked on Figure A.1.
b) “1, “3: 35 cm (14 in.) away from the air filter surface, measured at the center of horizontal line.
c) “2, “4: 61 cm (24 in.) away from the air filter surface, measured at the center of horizontal line.

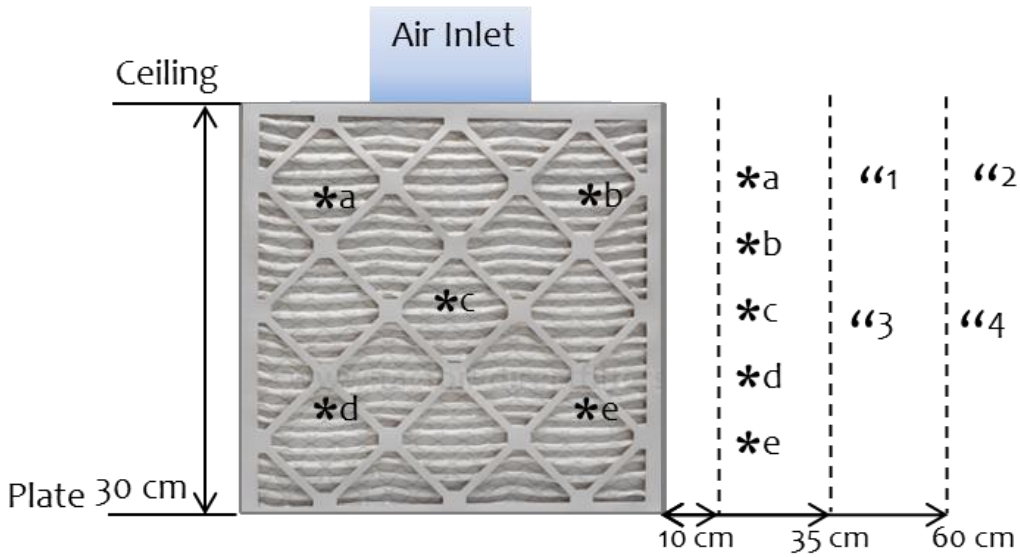

Figure B.1. Inlet air velocity measurement locations

Measured velocities are shown in Table A.1 as below for the two highest air flow rates.

Table B.1. Measured velocities for the two highest air flow rates

Location	Velocity(m/s)	
	161 CFM	273 CFM
*a	0.75	1.2
*b	0.7	1.2
*c	0.6	0.8
*d	0.75	1.2
*e	0.7	1.15
“1	0.2	
“2	0.2	
“3	0.7	
“4	0.5	

Appendix C. Characteristics of the Range Hoods

BROAN 42000 Series, Model 42301

This hood is an inverted "bowl" (Figure B.1). This hood is a basic low-cost model. The fan is an axial type mounted in the center of the hood. There is a single grease screen mounted at an angle in front of the fan. The grease screen dimensions are 25 cm x 21 cm (10 in. x 7.8 in.).

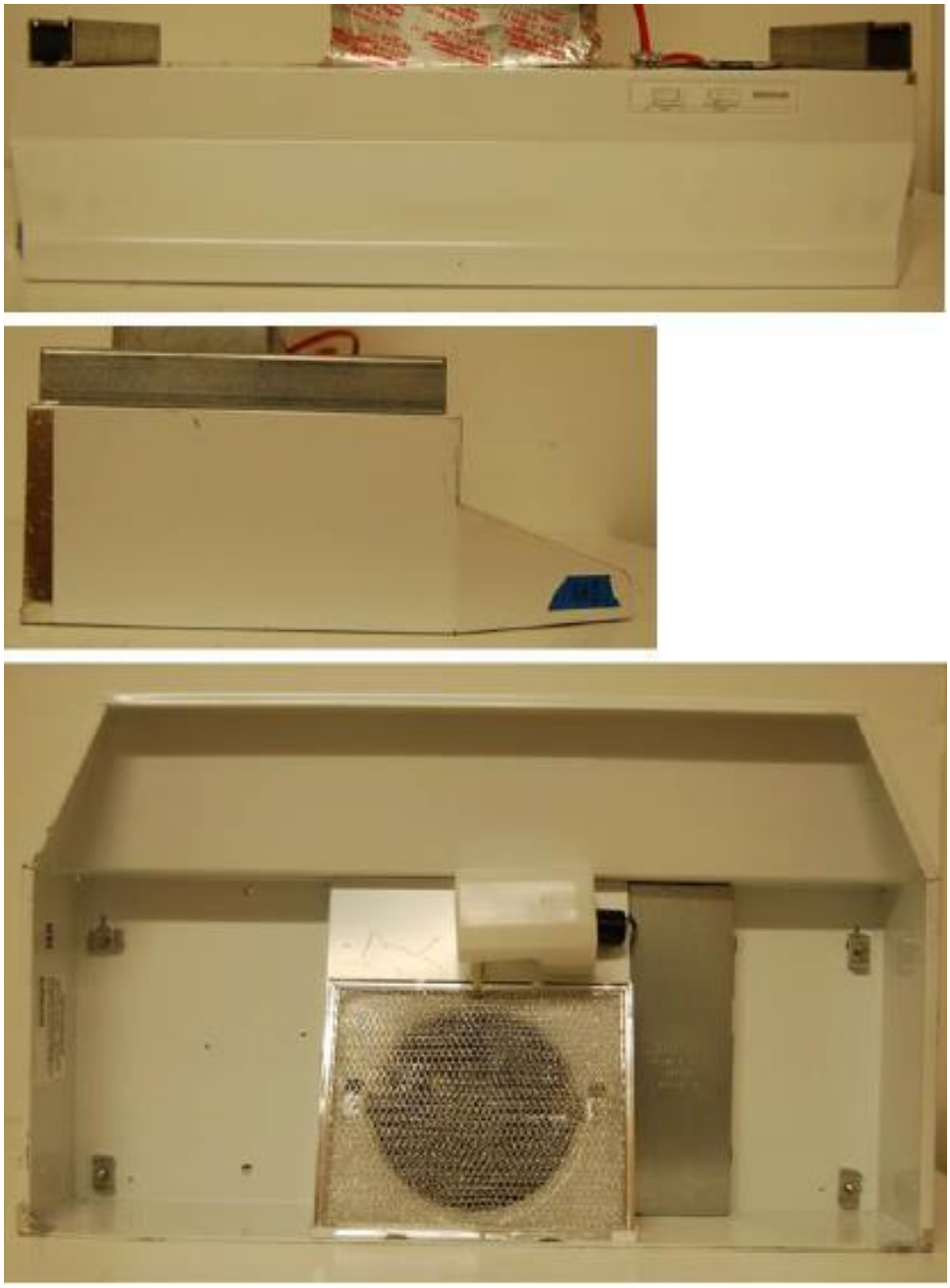

Figure C.1. BROAN 42000 Series, Model 42301

Vent-a-Hood, Model B100

This hood is an inverted "bowl" (Figure B.2). This hood is a basic unit that is advertised as being quieter than the entry-level modes. The fan is an axial type mounted in the center of the hood, housed in a box-like enclosure. There is a single grease screen mounted flush with the bottom of the hood. The grease screen dimensions are 28.5 cm x 29.5 cm (11.2 in. x 11.6 in.).

Figure C.2. Vent-a-Hood, Model B100

Appendix D. Results Summary

Table D.1 Range hood test results

Range Hood	Height (cm/in.)	Airflow (L/s/CFM)	Air Inlet	Burners	CO_2 concentration (ppm)	CE (%)
Broan	61/24	76/162	Old Inlet	Old F&B	2,000	85
Broan	46/18	76/162	Old Inlet	Old F&B	2,000	93
Broan	46/18	50/106	Old Inlet	Old F&B	2,000	80
Broan	61/24	50/106	Old Inlet	Old F&B	2,000	72
Vent-a-Hood	61/24	130/275	Old Inlet	Old F&B	2,000	99
Vent-a-Hood	69/27	130/275	Old Inlet	Old F&B	2,000	96
Vent-a-Hood	69/27	129/273	Old Inlet	New F&B	2,000	96
Vent-a-Hood	69/27	129/273	Old Inlet	New 2F	2,000	84
Vent-a-Hood	61/24	129/273	Old Inlet	New 2F	2,000	91
Vent-a-Hood	61/24	129/273	Old Inlet	New F&B	2,000	94
Broan	46/18	52/110	Old Inlet	New 2F	2,000	70
Broan	46/18	52/110	Old Inlet	New F&B	2,000	82
Broan	61/24	50/104	Old Inlet	New 2F	2,000	63
Broan	61/24	50/104	Old Inlet	New F&B	2,000	81
Broan	61/24	73/155	Old Inlet	New 2F	2,000	80
Broan	61/24	73/153	Old Inlet	New F&B	2,000	87
Broan	46/18	73/154	Old Inlet	New F&B	2,000	90
Broan	46/18	73/154	Old Inlet	New 2F	2,000	80
Broan	76/30	76/160	Old Inlet	New 2F	2,000	75
Broan	76/30	76/159	Old Inlet	New F&B	2,000	81
Broan	76/30	76/158	Old Inlet	Old F&B	2,000	79
Broan	61/24	50/106	Old Inlet	New 2F	2,000	64
Broan	46/18	50/107	Old Inlet	New 2F	2,000	70
Broan	46/18	75/158	Old Inlet	New 2F	2,000	81
Broan	61/24	73/154	Old Inlet	New 2F	2,000	70
Vent-a-Hood	61/24	132/279	Old Inlet	New 2F	2,000	96
Vent-a-Hood	61/24	131/278	Old Inlet	New 2F	3,000	85

Table D.1 (cont'd)

Range Hood	Height (cm/in.)	Airflow (L/s/CFM)	Air Inlet	Burners	CO_2 concentration (ppm)	CE (%)
Vent-a-Hood	61/24	132/280	Old Inlet	New 2F	2,000	94
Vent-a-Hood	61/24	132/278	Old Inlet	New 2F	2,000	90
Vent-a-Hood	61/24	132/284	Old Inlet	New 2F	2,000	93
Vent-a-Hood	61/24	132/280	Old Inlet	New 2F	2,000	87
Vent-a-Hood	61/24	132/279	Old Inlet	New 2F	3,000	87
Vent-a-Hood	61/24	132/280	Old Inlet	New 2F	2,000	94
Vent-a-Hood	61/24	132/279	Old Inlet	New 2F	3,000	94
Vent-a-Hood	61/24	132/280	Old Inlet	New 2F	2,000	94
Vent-a-Hood	61/24	132/280	Old Inlet	New 2F	3,000	93
Vent-a-Hood	61/24	134/283	Old Inlet	New 2F	2,000	91
Vent-a-Hood	61/24	132/280	Old Inlet	New 2F	2,000	86
Vent-a-Hood	61/24	132/280	Old Inlet 25 Gap	New 2F	2,000	96
Vent-a-Hood	61/24	132/280	Old Inlet 25 Gap	New 2F	3,000	96
Vent-a-Hood	61/24	132/281	Old Inlet 25 Gap	New 2F	2,000	98
Vent-a-Hood	61/24	134/283	Old Inlet 25 Gap	New 2F	3,000	99
Vent-a-Hood	61/24	131/278	Old Inlet 25 Gap	New 2F	2,000	96
Vent-a-Hood	61/24	132/280	Old Inlet 25 Gap	New 2F	3,000	96
Vent-a-Hood	61/24	131/278	Old Inlet 25 Gap	New 2F	2,000	96
Vent-a-Hood	61/24	132/279	Old Inlet 25 Gap	New 2F	3,000	97

Table D.1 (cont'd)

Range Hood	Height (cm/in.)	Airflow (L/s/CFM)	Air Inlet	Burners	CO_2 concentration (ppm)	CE (%)
Vent-a-Hood	69/27	130/276	Old Inlet 25 Gap	New 2F	2,000	96
Vent-a-Hood	69/27	131/278	Old Inlet 25 Gap	New 2F	3,000	96
Vent-a-Hood	69/27	132/280	Old Inlet 25 Gap	New 2F	2,000	96
Vent-a-Hood	69/27	132/280	Old Inlet 25 Gap	New 2F	3,000	96
Broan	61/24	75/159	Old Inlet 25 Gap	New 2F	3,000	84
Broan	61/24	74/157	Old Inlet 25 Gap	New 2F	2,000	85
Broan	61/24	74/157	Old Inlet 25 Gap	New F&B	2,000	89
Broan	61/24	74/157	Old Inlet 25 Gap	Old F&B	2,000	79
Broan	46/18	74/158	Old Inlet 25 Gap	New 2F	2,000	89
Broan	46/18	74/158	Old Inlet 25 Gap	New 2F	3,000	89
Broan	46/18	74/158	Old Inlet 25 Gap	New F&B	2,000	95
Broan	46/18	74/157	Old Inlet 25 Gap	Old F&B	2,000	87
Broan	61/24	74/158	Old Inlet	New 2F	2,000	79
Broan	61/24	74/156	Old Inlet	New F&B	2,000	85
Broan	61/24	74/156	Old Inlet	Old F&B	2,000	74
Broan	46/18	76/161	Old Inlet	New 2F	2,000	77
Broan	46/18	76/161	Old Inlet	New F&B	2,000	84
Broan	46/18	76/161	Old Inlet	Old F&B	2,000	79
Broan	46/18	76/161	New Inlet	New 2F	2,000	89
Broan	46/18	76/161	New Inlet	New F&B	2,000	95
Broan	46/18	76/161	New Inlet	Old F&B	2,000	88
Broan	61/24	76/161	New Inlet	New 2F	2,000	87
Broan	61/24	76/161	New Inlet	New F&B	2,000	92
Broan	61/24	76/161	New Inlet	Old F&B	2,000	80
Broan	61/24	76/161	New Inlet	New F & B	2,000	92

Table D.1 (cont'd)

Range Hood	Height (cm/in.)	Airflow (L/s/CFM)	Air Inlet	Burners	CO_2 concentration (ppm)	CE (%)
Vent-a-Hood	61/24	129/273	New Inlet	New 2F	2,000	95
Vent-a-Hood	61/24	129/273	New Inlet	New F&B	2,000	99
Vent-a-Hood	61/24	127/270	New Inlet	Old F&B	2,000	98
Vent-a-Hood	69/27	129/273	New Inlet	New F&B	2,000	99
Vent-a-Hood	69/27	129/273	New Inlet	New 2F	2,000	90
Vent-a-Hood	69/27	127/270	New Inlet	Old F&B	2,000	97
Broan	61/24	50/105	New Inlet	New 2F	2,000	63
Broan	61/24	50/105	New Inlet	New F&B	2,000	74
Broan	61/24	50/105	New Inlet	Old F&B	2,000	59
Broan	46/18	50/105	New Inlet	New F&B	2,000	78
Broan	46/18	50/105	New Inlet	Old F&B	2,000	65

Appendix E. Capture Efficiency Step-by-Step Testing Procedure

1. Install the range hood above the cooktop and adjust the position to target the height above the cooktop.
2. Start the data acquisition system (laptop software) to measure airflow and record CO_2 concentrations and cooktop power.
3. Start the temperature data loggers, to record the emitter surface temperatures.
4. Turn on the range hood and adjust the airflow rate to the target test airflow.
5. Place the emitters on the electric heating element and turn on the heating element (target power is 1 kilowatt [kW] for each element)
6. Ensure that the test chamber door is air sealed.
7. Wait until the surface temperature reaches to target temperature and is stabilized (200°C [392°F] ± 5°C).
8. Open the valve to inject CO_2 tracer gas into the tracer gas emitters. Use a mass flow controller to achieve approximately 2,000 ppm at the exhaust.
9. Wait until the steady-state condition is achieved (four air changes).
10. Record the CO_2 concentrations for at least 10 minutes.
11. Calculate the capture efficiency, using these averaged values, with Equation 1.